Supporting information

Controlling fluorescence resonance energy transfer of donor-acceptor dyes by Diels-Alder dynamic covalent bonds

Yanhui Cui, Fen Li, and Xin Zhang*

School of Chemical Engineering and Technology, Collaborative Innovation Center of Chemistry Science and Engineering, Tianjin University, Tianjin 300072, China

Email: xzhangchem@tju.edu.cn

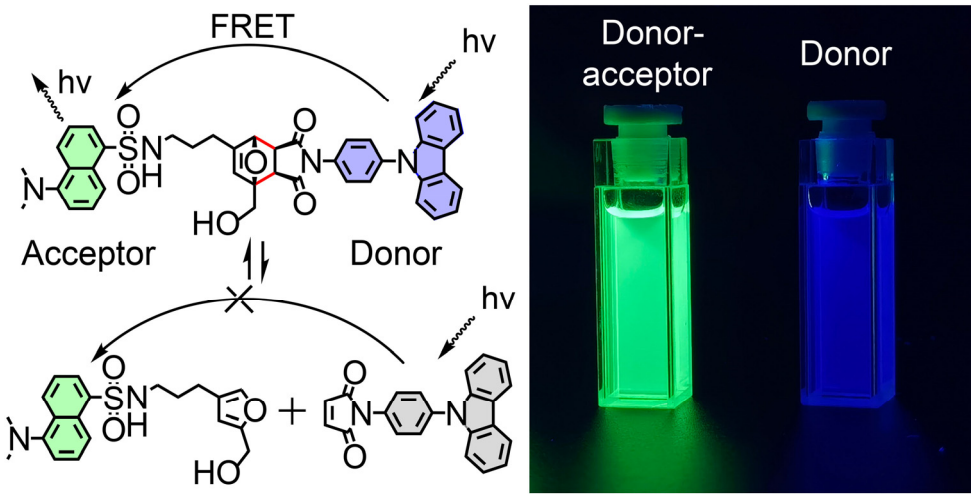

Two new dyes consisting of aromatic amine donor and dansyl acceptor were synthesized, where intramolecular donor and acceptor are connected by Diels-Alder dynamic covalent bonds. These new dyes display a switchable fluorescence resonance energy transfer through reversible formation and cleavage of Diels-Alder bonds. Single crystal X-ray diffraction revealed that Diels-Alder bonds are longer and weaker than normal single bonds. Dynamic covalent properties enable the mutual conversion of the two dyes by maleimide exchanges, where new higher energy transfer efficiency system can be constructed.

Table of Contents

1. Materials and methods

^{1}H NMR, ^{13}C NMR spectra were acquired on a Bruker 600MHz NMR instrument using $CDCl_3$ as a solvent in room temperature and tetramethylsilane as an internal standard. Infrared spectra were recorded on a Bruker ALPHA II FTIR spectrometer. High resolution mass spectra (HRMS) were obtained on a Bruker miorOTOF-QII using ESI. UV-vis absorption spectra were measured on an Agilent Varian Cary 300 spectrophotometer. The extinction coefficient (ε) was calculated according to Lambert-Beer's law. Steady-state fluorescence spectra were recorded on a FLS980 fluorescence spectrophotometer at room temperature. All solvents used for spectral measurements are spectrally pure and used without further purification unless otherwise stated.

The fluorescence lifetimes were measured at the room temperature by using the Edinburgh instruments FLS980. The response of the instrument was measured with 30% silica suspension solution using nanosecond flash lamp as pulse light source. Fluorescence quantum yields were calculated using the following equation:

$$\Phi = \Phi_r \frac{I}{I_r} \frac{A_r}{A} \frac{n^2}{{n_r}^2}$$

where I and I_r are the integral regions under the emission bands of the samples and the reference solution, respectively. A and A_r are the absorbance of the samples and the reference solution respectively. n and n_r are the refractive indices of the samples and the reference solvent, respectively. The quinine sulfate in sulfuric acid aqueous solution (Φ_r=0.55) was chosen as a reference. [1]

2. Synthesis and characterization

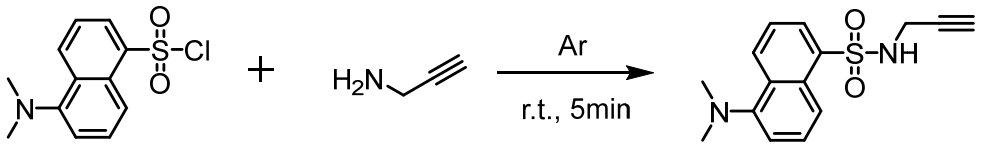

5-(dimethylamino)-N-(prop-2-yn-1-yl)naphthalene-1-sulfonamide: Propargyl amine (0.11 g, 1.2 mmol) was dissolved in dry dichloromethane (2 ml) in argon atmosphere. The dichloromethane solution (10 ml) of dansyl chloride (0.27 g, 1 mmol) was dropwise added into the above solution, and the reaction was carried out at room temperature for 5 min. Crude product was purified by silica gel column chromatography (ethyl acetate/petroleum ether = 1/3 (v/v)) to give yellow green oil (0.27 g, 0.94 mmol, 94%).

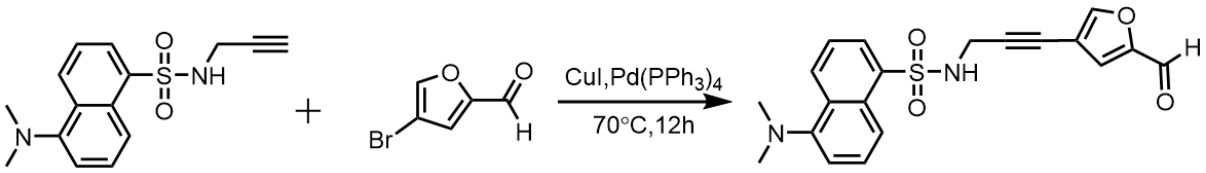

5-(dimethylamino)-N-(3-(5-formylfuran-3-yl)prop-2-yn-1-yl)naphthalene-1-sulfonamid e: 5-(dimethylamino)-N-(prop-2-yn-1-yl)naphthalene-1-sulfonamide (0.2 g, 1.2 mmol) and 4-bromofuran-2-carbaldehyde (0.28 g, 1 mmol) were dissolved in dry tetrahydrofuran (5 ml)/triethylamine (5 ml) in argon atmosphere. Cuprous iodide (0.0095 g, 0.05 mmol), tetrakis (triphenylphosphine) palladium (0.058 g, 0.05mmol) were added and heated to 70 ℃ under stirring for 12 h. The reaction mixtures were then washed by water and extracted by dichloromethane (30 ml × 3). The crude product was purified by silica gel column chromatography (ethyl acetate/petroleum ether = 1/2 (v/v)) to give the yellow oil (0.14 g, 0.37 mmol, 37%).

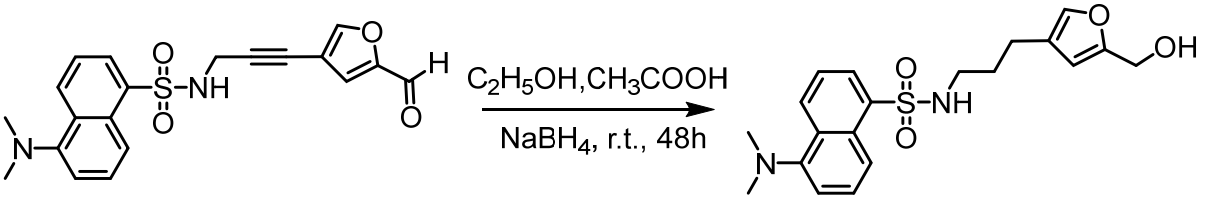

3

Acceptor 3: 5-(dimethylamino)-N-(3-(5-formylfuran-3-yl)prop-2-yn-1-yl) naphthalene- 1-sulfonamide (0.2 g, 0.52 mmol) was dissolved in absolute ethanol (15 ml) and acetic acid (1 ml), then Pd/C (0.03 g, 10%, WT) was added. Sodium borohydride (0.2 g) was added into the above reaction mixtures. The reaction was performed for 48 h at room temperature. After the filtration and extraction of reaction mixtures, the crude product was purified by silica gel column chromatography (dichloromethane/ethyl acetate=10/1 (v/v)) to give yellow oil (0.13 g, 0.33 mmol, 62%).

^{1}H NMR (600 MHz, $CDCl_3$, Figure S1): δ = 8.56-8.51 (d, *J* = 3.0 Hz, 1H, ArH), δ = 8.31-8.27 (d, *J* = 2.4 Hz, 1H, ArH), δ = 8.25-8.21 (d, *J* = 2.4 Hz, 1H, ArH), δ = 7.60-7.49 (m, 2H, ArH), δ = 7.22-7.17 (d, *J* = 3.0 Hz, 1H, ArH), δ = 6.93-6.90 (s, 1H, -CR=CH-), δ = 5.96-5.91 (s, 1H, -O-CH=CR-), δ = 4.79-4.69 (t, *J* = 6.0 Hz, 1H, -SO2-NH-), δ = 4.54-4.45 (d, *J* = 5.4 Hz, 2H, -CR-CH2-O-), δ = 2.94-2.85 (m, 8H, -NR-CH2-, 2-CH3), δ = 2.30-2.23 (t, *J* = 4.2 Hz, 2H, -CR-CH2-), δ = 1.90-1.83 (t, *J* = 4.2 Hz, 1H, -OH), δ = 1.66-1.56 (m, 2H, -CH2-).
^{13}C NMR ($CDCl_3$, Figure S2): δ = 154.31, 152.10, 138.94, 134.68, 130.54, 129.95, 129.84, 129.68, 128.52, 124.40, 123.32, 118.76, 115.29, 108.93, 57.63, 45.52, 42.61, 29.71, 21.64.
IR (KBr pellet, cm^{-1}): 3433.80, 3178.96, 2925.74, 2864.26, 2791.50, 1709.06, 1574.59, 1453.31, 1399.58, 1304.23, 1136.30, 1081.65, 1003.48, 965.31, 946.25, 915.93, 820.00, 785.42, 753.08, 682.77.
HRMS: m/z calculated for $C_{20}H_{24}N_2O_4S$: $[M+H]^+$: 389.1535, found: 389.1538.

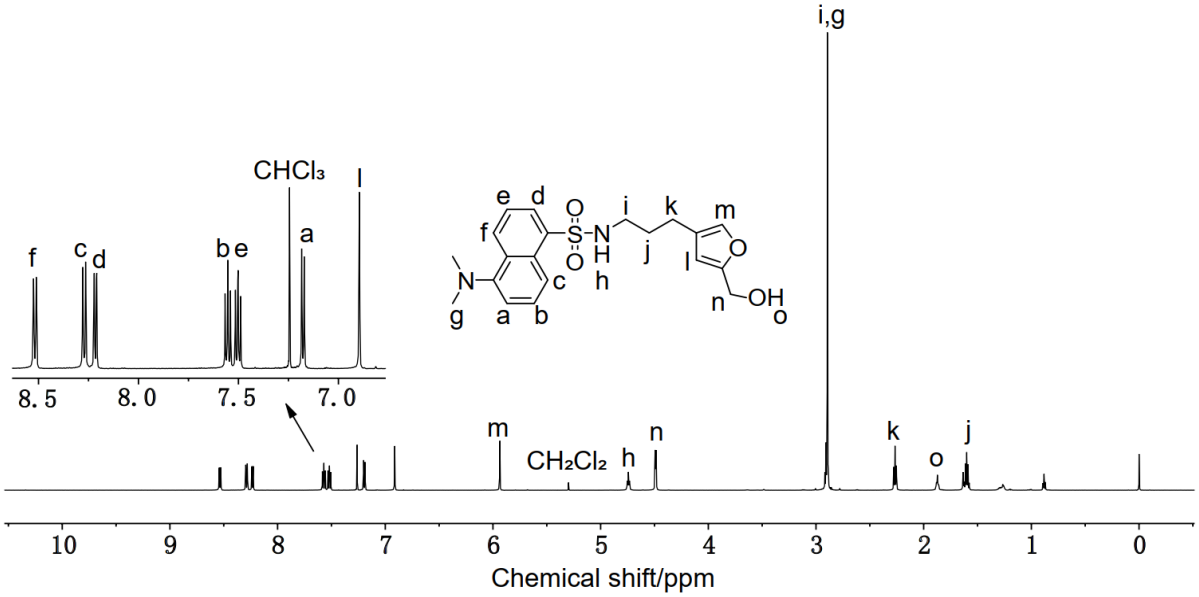

Figure S1. ^{1}H NMR spectrum of **3** in $CDCl_3$ with corresponding signal assignments and its chemical structure.

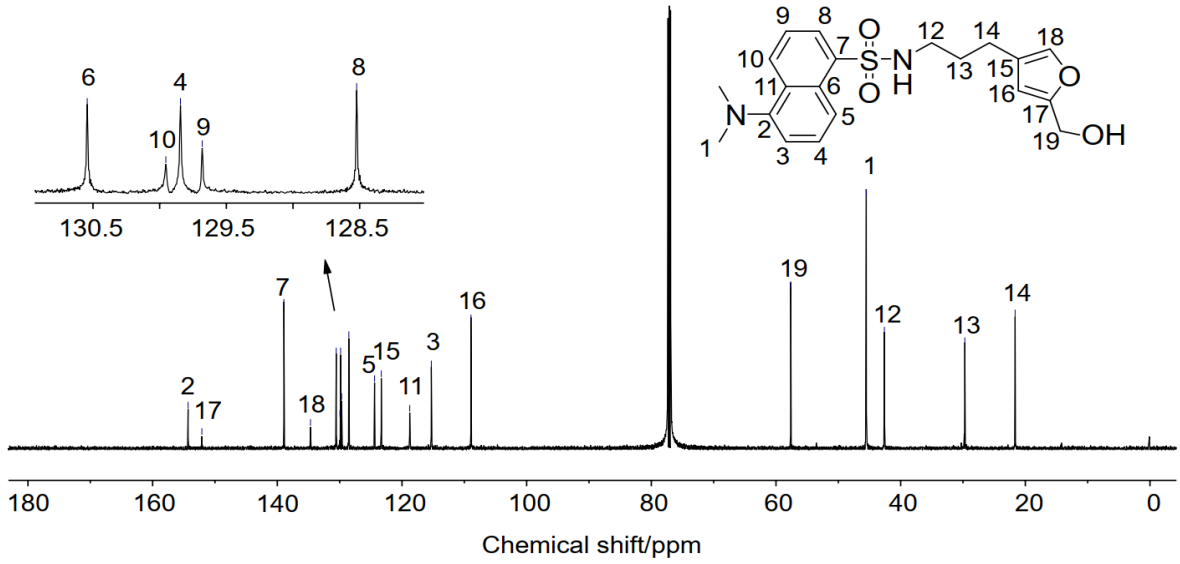

Figure S2. ^{13}C NMR spectrum of **3** in $CDCl_3$ with corresponding signal assignments and its chemical structure.

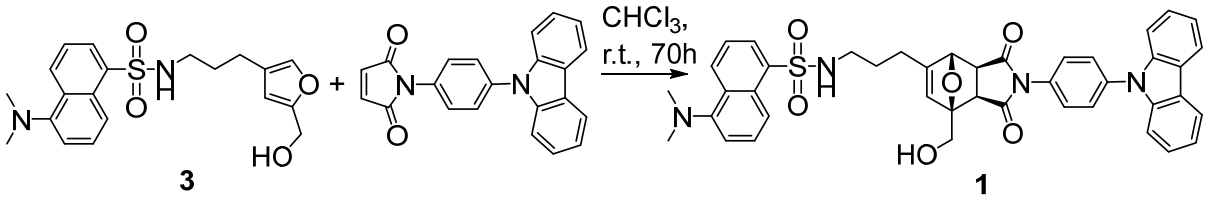

Donor-acceptor 1: Acceptor **3** (0.19 g, 0.6 mmol) and triphenylamine-based maleimide (0.17 g, 0.5 mmol) were dissolved in chloroform (5 mL) and stirred at room temperature for 70 h.[2] The reaction mixtures were washed with deionized water and extracted by dichloromethane for three times. After being concentrated, the crude product was purified by silica gel column chromatography with ethyl acetate/n-hexane (1/3, v/v) as eluent to give yellow green oil (0.15 g, 0.21 mmol). Yield: 41%.

^{1}H NMR (600 MHz, $CDCl_3$, Figure S3): δ = 8.59-8.55 (d, *J* = 2.4 Hz, 1H, ArH), δ = 8.30-8.25 (t, *J* = 3.0 Hz, 2H, ArH), δ = 8.16-8.13 (d, *J* = 1.8 Hz, 2H, ArH), δ = 7.72-7.68 (d, *J* = 2.4 Hz, 2H, ArH), δ = 7.62-7.56 (m, 2H, ArH), δ = 7.55-7.53 (d, *J* = 1.2 Hz, 2H, ArH), δ = 7.49-7.46 (d, *J* = 1.8 Hz, 2H, ArH), δ = 7.44-7.40 (t, *J* = 2.4 Hz, 2H, ArH), δ = 7.33-7.29 (t, *J* = 2.4 Hz, 2H, ArH), δ =7.23-7.20 (d, *J* = 1.8 Hz, 1H, ArH), δ = 6.07-6.04 (s, 1H, -CR=CH-), δ = 5.06-5.03 (s, 1H, -O-CRH-), δ = 4.70-4.64 (t, *J* = 3.6 Hz, 1H, -SO2-NH-), δ = 4.16-4.09 (d, *J* = 4.2 Hz, 2H, -CR-CH2-O-), δ = 3.15-3.12 (d, *J* = 1.8 Hz, 1H, -CRH-), δ = 3.09-3.06 (d, *J* = 1.8 Hz, 1H, -CRH-), δ = 3.02-2.88 (m, 8H, -NR-CH2-, 2-CH3), δ = 2.68-2.64 (t, *J* = 2.4 Hz, 1H, -OH), δ = 2.25-2.20 (t, *J* = 3.0 Hz, 2H, -CR-CH2-), δ = 1.70-1.62 (m, 2H, -CH2-).

^{13}C NMR ($CDCl_3$, Figure S6): δ = 175.14, 152.26, 151.53, 140.59, 138.13, 134.64, 130.75, 130.23, 129.97, 129.84, 129.64, 128.68, 128.02, 127.57, 126.20, 123.63, 123.37, 120.46, 120.40, 118.60, 115.40, 109.84, 92.75, 83.52, 61.12, 49.85, 49.62, 45.51, 42.51, 26.86, 24.17.

IR (KBr pellet, cm^{-1}): 3549.65, 3279.52, 2943.54, 2788.52, 1777.01, 1706.72, 1602.92, 1573.96, 1515.54, 1478.40, 1451.93, 1393.43, 1357.75, 1317.04, 1186.50, 1160.91, 1140.82, 1071.38, 944.77, 837.95, 791.80, 749.87, 724.78, 682.25.

HRMS: m/z calculated for $C_{42}H_{38}N_4O_6S$: $[M-H]^-$: 725.2439, found: 725.2432.

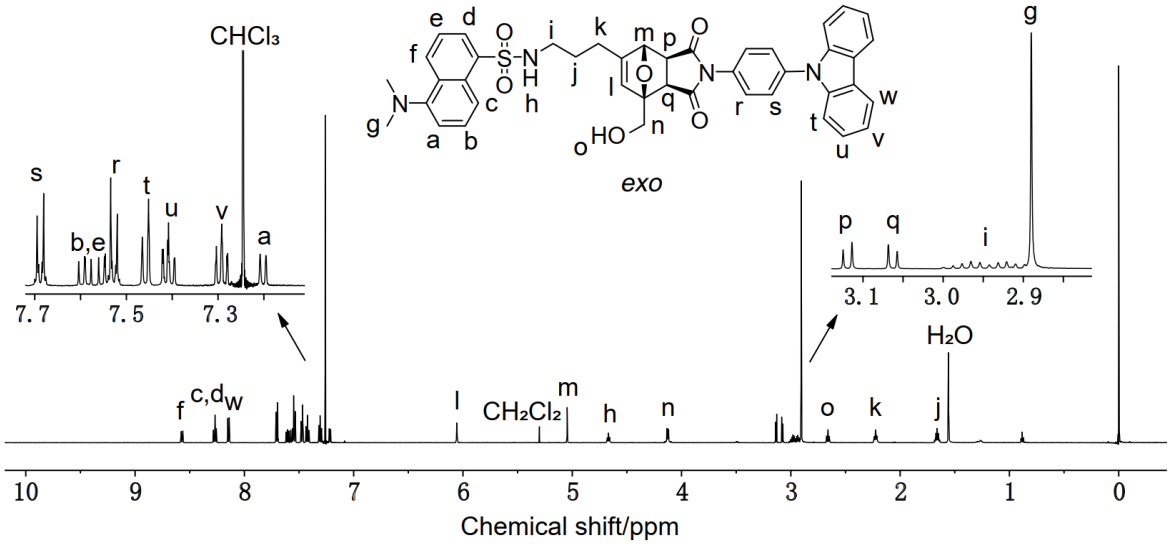

Figure S3. ^{1}H NMR spectrum of *exo*-**1** in $CDCl_3$ with corresponding signal assignments and its chemical structure.

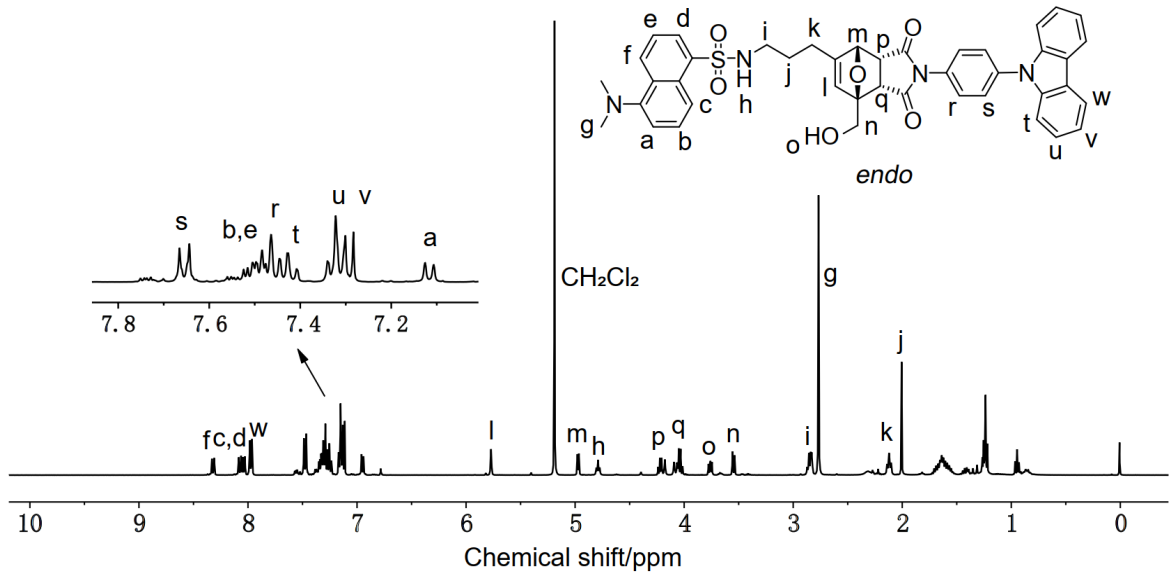

Figure S4. ^{1}H NMR spectrum of *endo*-**1** in $CDCl_3$ with corresponding signal assignments and its chemical structure.

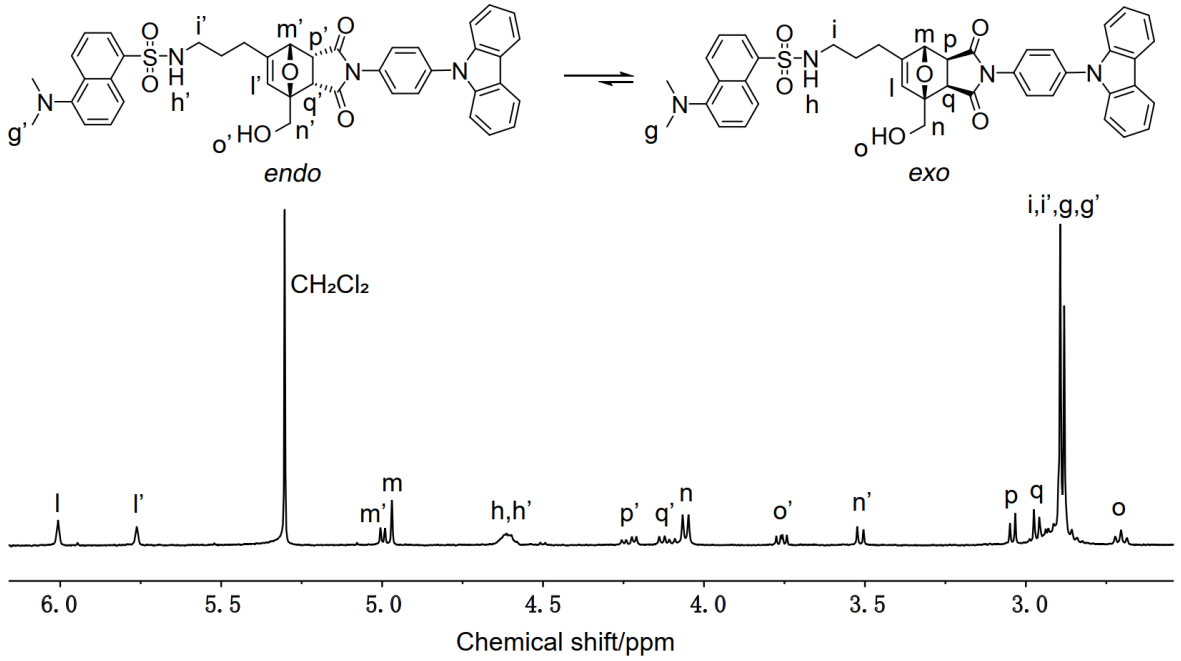

Figure S5. ^{1}H NMR spectrum of the mixture of *exo*-**1** and *endo*-**1** in $CDCl_3$ with corresponding signal assignments and their chemical structures. The ratio of exo isomer to endo isomer is about 7: 3 at 48 h of Diels-Alder reaction.

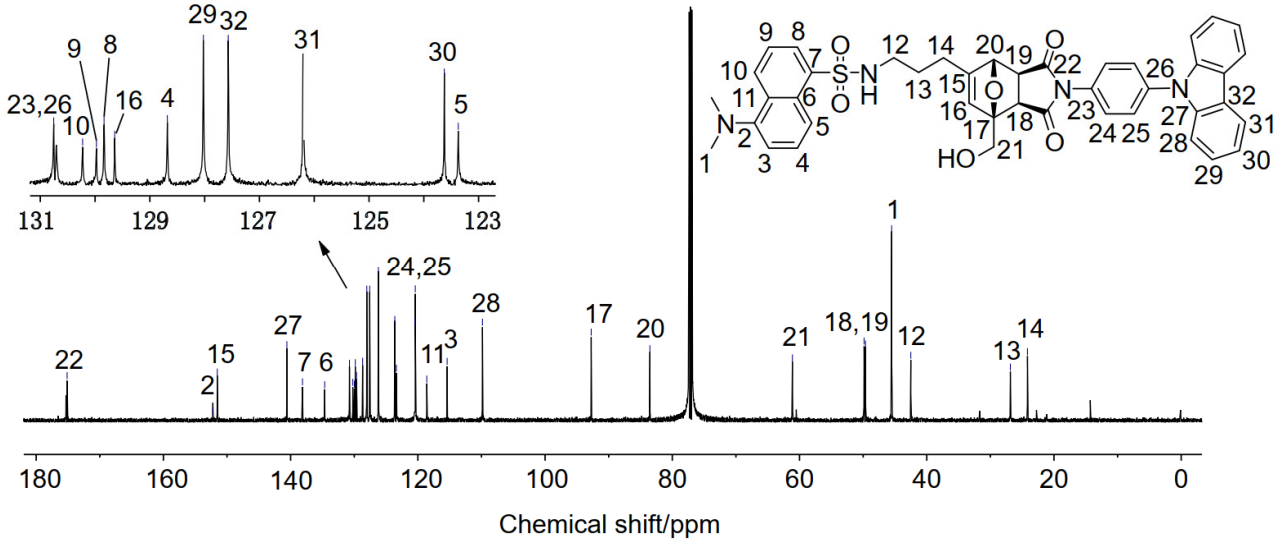

Figure S6. ^{13}C NMR spectrum of *exo*-**1** in $CDCl_3$ with corresponding signal assignments and its chemical structure.

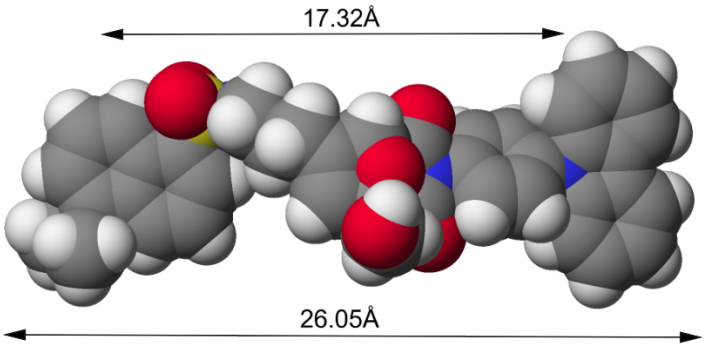

Figure S7. Energy-optimized molecular structure of **1** calculated by AM 1 semi-empirical method.

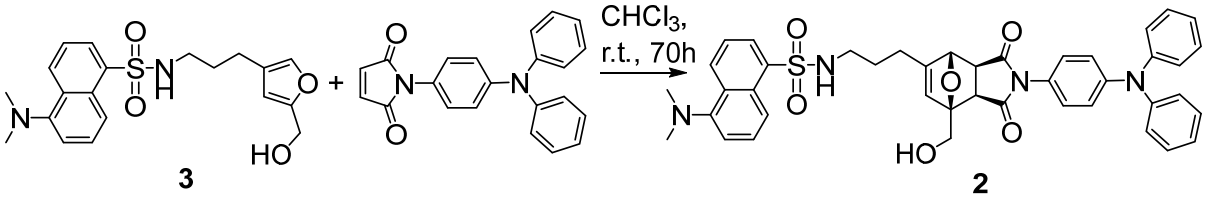

3 **2**

Donor-acceptor **2** was synthesized from carbazole-based maleimide in the same manner as **1**. The crude product was purified by silica gel column chromatography with ethyl acetate/n-hexane (1/2, v/v) as eluent to give yellow green oil (0.20 g, 0.27 mmol). Yield: 54%.

^{1}H NMR (600 MHz, $CDCl_3$, Figure S8): δ = 8.58-8.53 (d, *J* = 3.0 Hz, 1H, ArH), δ = 8.29-8.23 (t, *J* = 3.6 Hz, 2H, ArH), δ = 7.61-7.52 (m, 2H, ArH), δ = 7.32-7.24 (m, 4H, ArH), δ = 7.22-7.18 (d, *J* = 2.4 Hz, 1H, ArH), δ =7.15-7.04 (m, 10H, ArH), δ = 6.02-5.99 (s, 1H, -CR=CH-), δ = 4.98-4.95 (s, 1H, -O-CRH-), δ = 4.70-4.64 (t, *J* = 3.6 Hz, 1H, -SO2-NH-), δ = 4.09-4.03 (d, *J* = 3.6 Hz, 2H, -CR-CH2-O-), δ = 3.05-2.95 (m, 2H, -CRH-CRH-), δ = 2.95-2.86 (m, 8H, -NR-CH2-, 2-CH3), δ = 2.73-2.68 (t, *J* = 3.0 Hz, 1H, -OH), δ = 2.22-2.13 (t,

J = 5.4 Hz, 2H, -CR-CH2-), δ = 1.67-1.59 (m, 2H, -CH2-).

^{13}C NMR ($CDCl_3$, Figure S9): δ = 175.52, 152.20, 151.42, 148.30, 147.26, 134.67, 130.72, 129.95, 129.83, 129.81, 129.63, 129.51, 128.65, 127.18, 125.12, 123.72, 123.35, 122.69, 118.58, 115.37, 92.56, 83.37, 61.14, 49.69, 49.41, 45.51, 42.50, 26.84, 24.15.

IR (KBr pellet, cm^{-1}): 3479.74, 3291.44, 2940.69, 2781.71, 1774.67, 1702.86, 1588.47, 1507.70, 1489.71, 1391.27, 1316.63, 1278.96, 1187.05, 1160.16, 1141.89, 1073.60, 975.49, 943.82, 876.21, 828.78, 790.11, 754.06, 696.29.

HRMS: m/z calculated for $C_{42}H_{40}N_4O_6S$: $[M-H]^-$: 727.2596, found: 727.2588.

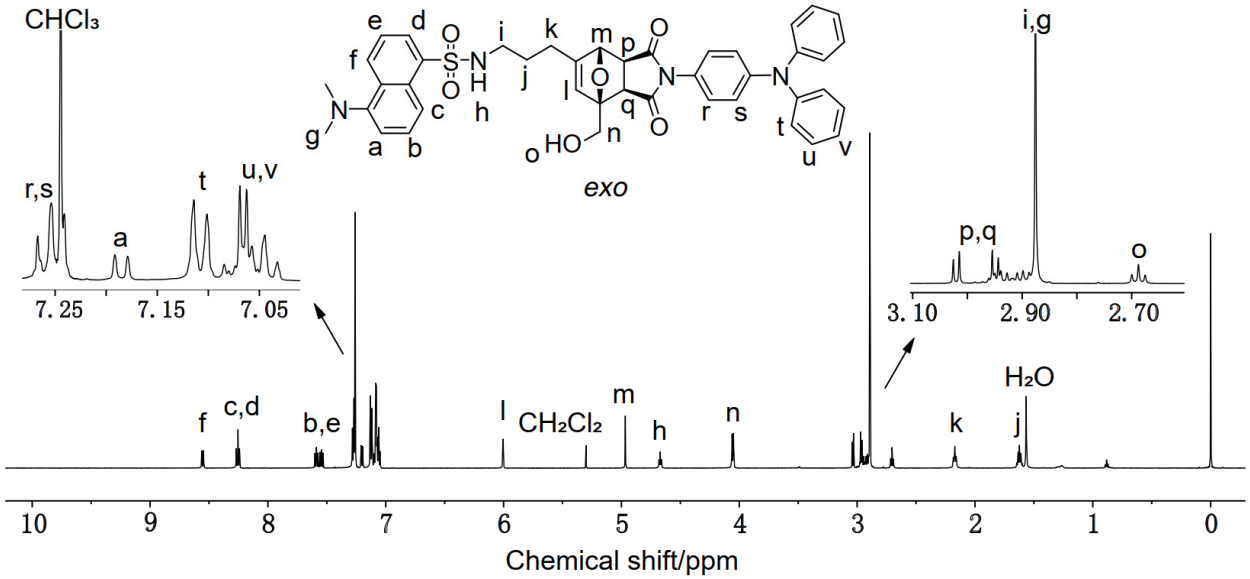

Figure S8. ^{1}H NMR spectrum of *exo*-**2** in $CDCl_3$ with corresponding signal assignments and its chemical structure.

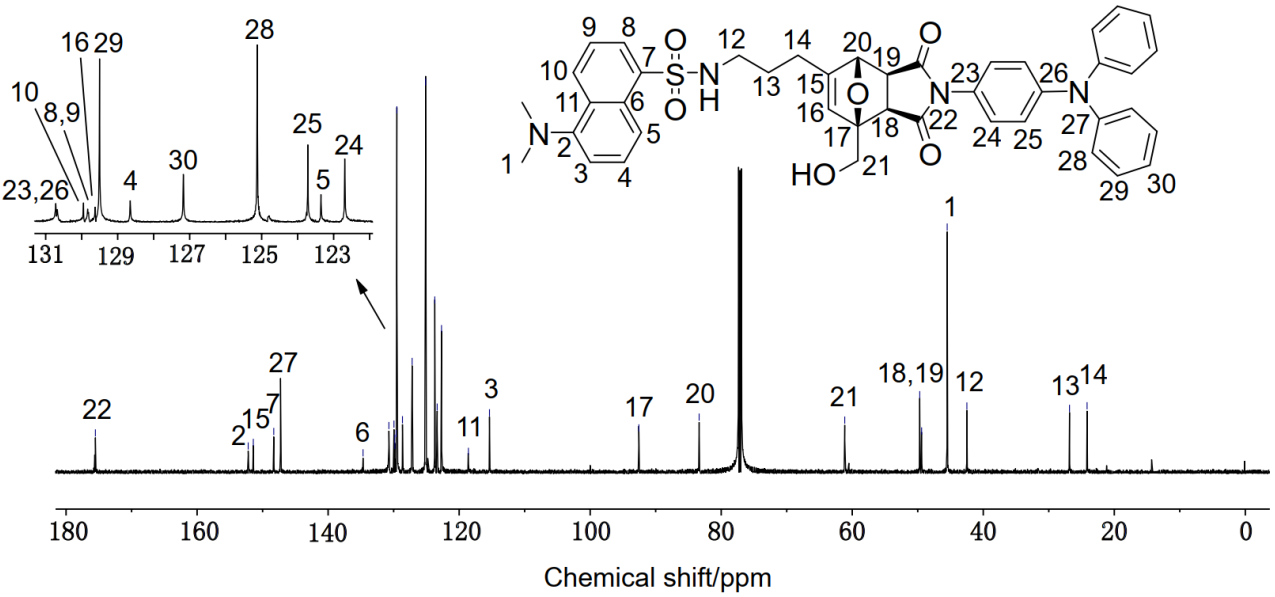

Figure S9. ^{13}C NMR spectrum of *exo*-**2** in $CDCl_3$ with corresponding signal assignments and its chemical structure.

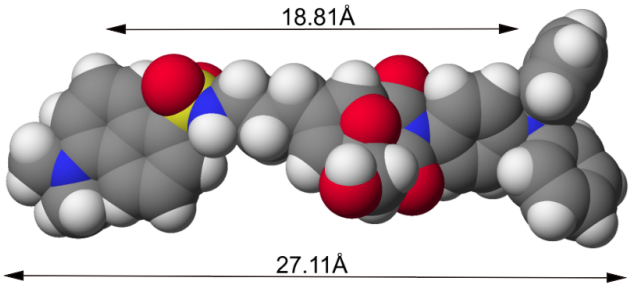

Figure S10. Energy-optimized molecular structure of **2** calculated by AM 1 semi-empirical method.

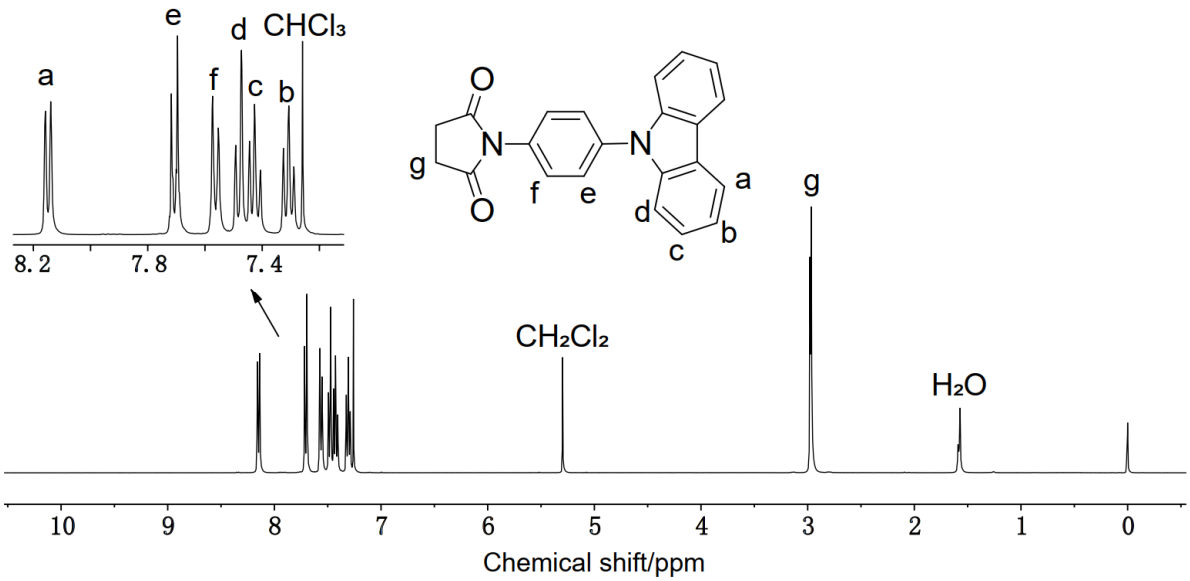

Figure S11. ^{1}H NMR spectrum of **4** in $CDCl_3$ with corresponding signal assignments and its chemical structure.

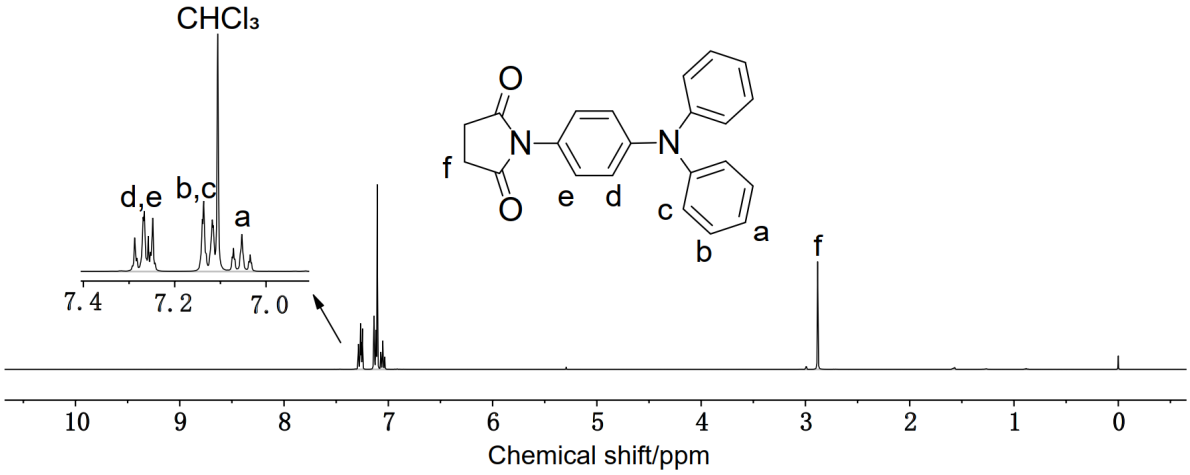

Figure S12. ^{1}H NMR spectrum of **5** in $CDCl_3$ with corresponding signal assignments and its chemical structure.

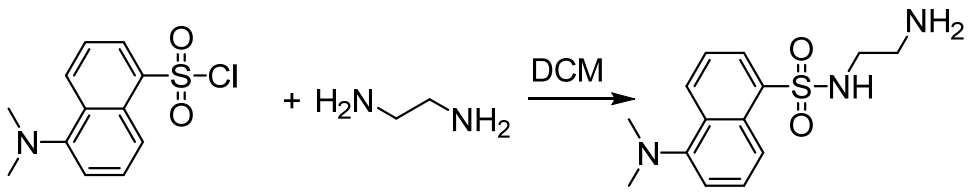

Ethylenediamine (0.74 ml, 11.1 mmol) and dry dichloromethane (5 ml) was added into a 100 ml round bottom flask at 0^0C with stirring. Dry dichloromethane solution (2 ml) of dansyl chloride (0.37 g) was slowly added to the above reaction mixture with stirring for 0.5 h at 0^0C, then the reaction was performed at room temperature with stirring for 1 h. Subsequently, hydrochloric acid solution (24 ml, 1M) was added into the reaction mixtures for acidification, and then extracted with dichloromethane. The organic phase obtained was dried with anhydrous magnesium sulfate, concentrated and dried in vacuum, then directly used for the next step reaction without further purification.

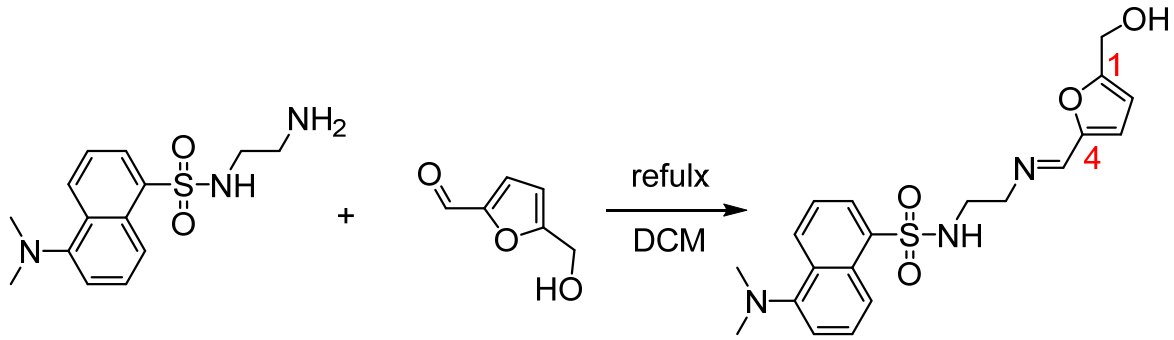

The above product (86 mg, 0.30 mmol) and 5-hydroxymethyl-2-furfuraldehyde (45 mg, 0.36 mmol) were added into a 50 ml round bottom flask in argon atmosphere. Dry dichloromethane (5 ml) and dry triethylamine (0.2 ml) were then added into the above reaction mixtures. The reaction was performed for 3 h. The crude product was purified by silica gel column chromatography (ethyl acetate / methanol = 10 / 1) to give the light green solid. A small amount of tetrahydrofuran was added to dissolve the product, and 20 ml of n-hexane was added for precipitation. The filtered light green powder was dried in vacuum. The yield: 34%.

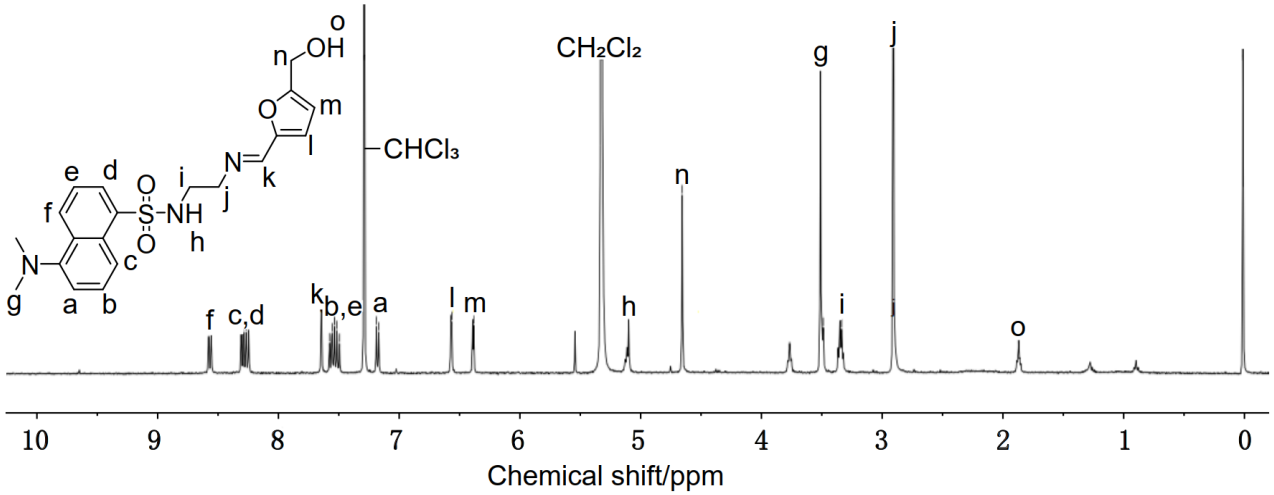

Figure S13. ^{1}H NMR spectrum of 1,4-substituted furan derivatives in $CDCl_3$ with corresponding signal assignments and its chemical structure.

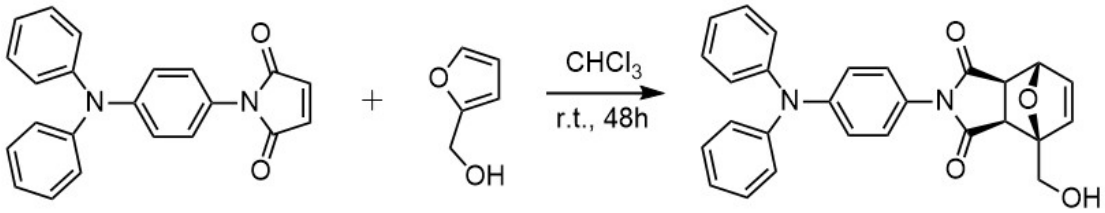

Model compound **M**: Triphenylamine-based maleimide (100mg, 0.29mmol) and furan methanol (40mg, 0.41mmol) were dissolved in 5mL trichloromethane, and the reaction was performed for 48h at room temperature, after the reaction was completed, the crude product was purified by silica gel column chromatography (ethyl acetate / petroleum ether = 1 / 2) to give the white solid. Yield: 40%. ^{1}H NMR (400 MHz, CDCl3): δ = 7.29 - 7.25 (m, 4H), 7.18 - 6.98 (m, 10H), 6.66 (d, J = 5.7 Hz, 1H), 6.58 (d, J = 5.7 Hz, 1H), 5.37 (s, 1H), 4.15 (s, 2H), 3.12 (q, J = 6.6 Hz, 2H).

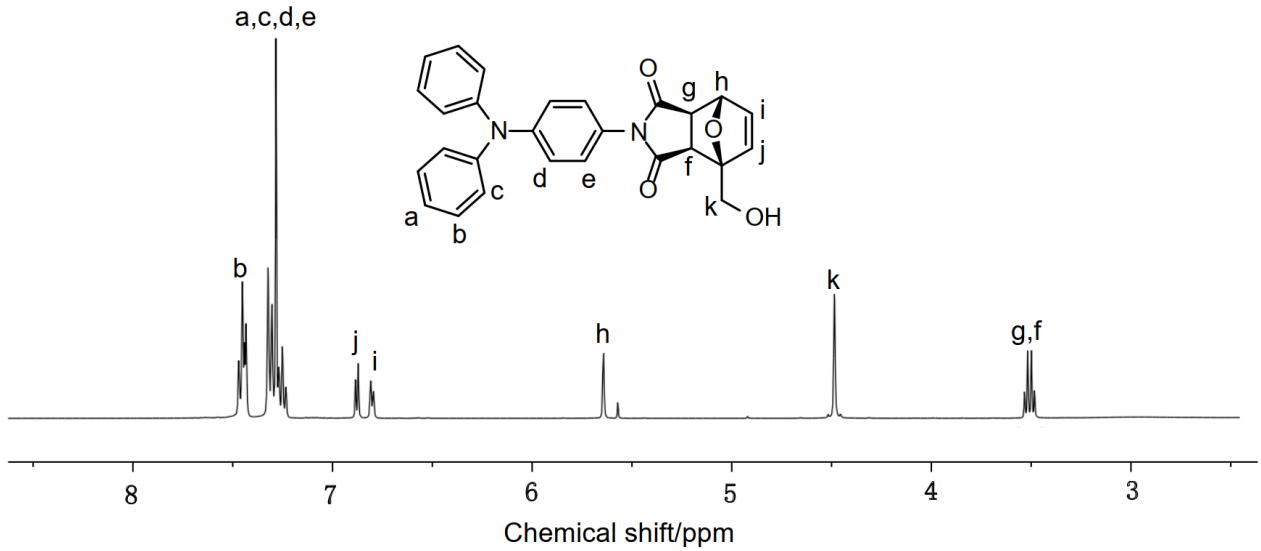

Figure S14. ^{1}H NMR spectrum of the model compound **M** in $CDCl_3$ with corresponding signal assignments and its chemical structure.

3. Single-crystal X-ray diffraction analysis

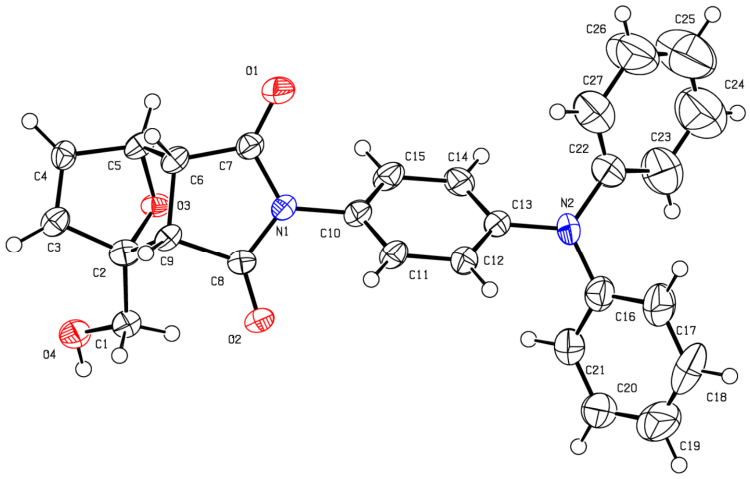

Figure S15. Molecular structure (ORTEP) of the model compound of **2** determined by single-crystal X-ray diffraction.

Table S1. Crystal data and structure refinement for the model compound **M**.

Identification code	**M**
Empirical formula	$C_{27}H_{22}N_2O_4$
Formula weight	438.46 g/mol
Temperature	113 K
Wavelength	0.71073 Å
Crystal system	monoclinic
space group	$P2_1$
Unit cell dimensions	a = 5.3407(11) Å α = 90.00°
	b = 12.745 (3) Å β =92.51 (3)°
	c = 18.872 (4) Å γ = 90.00°
Volume	1283.3 (4) $Å^3$
Z	2
Calculated density	1.135 Mg/m^3
Absorption coefficient	0.077 mm^{-1}
F (000)	460.0
Crystal size	0.20 × 0.18 × 0.12 mm^3
Theta (max)	27.850°
Limiting indices	-7<=h<=7, -16<=k<=16, -24<=l<=24
Reflections collected / unique	13184/3160 [R (int) = 0.0374]
Completeness to theta = 27.850	1.00/0.52
Max. and min. transmission	0.991 and 0.985
Refinement method	Full matrix least square F^2
Data / restraints / parameters	3160/1/276
Goodness-of-fit on F^2	1.040
R indices (all data)	R_1 = 0 .0709, wR_2 = 0.1968

4. UV-vis absorption and fluorescence spectroscopy

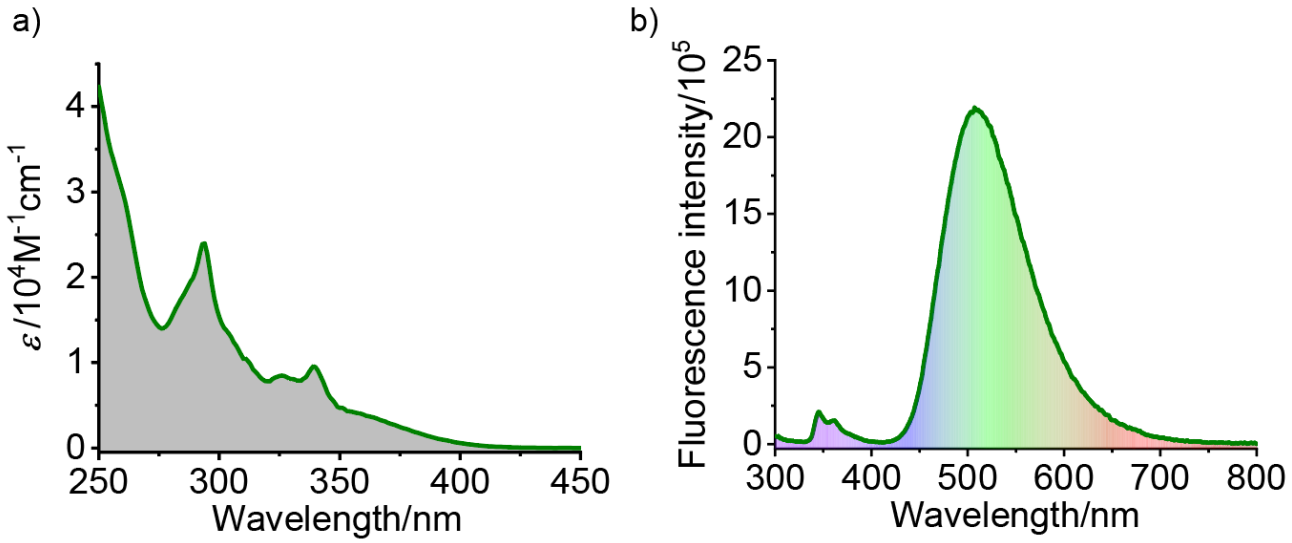

Figure S16. UV-vis absorption (a) and fluorescence spectra (b) of **1** in dichloromethane, c = $5x10^{-5}$ M. λ_{ex} = 294 nm.

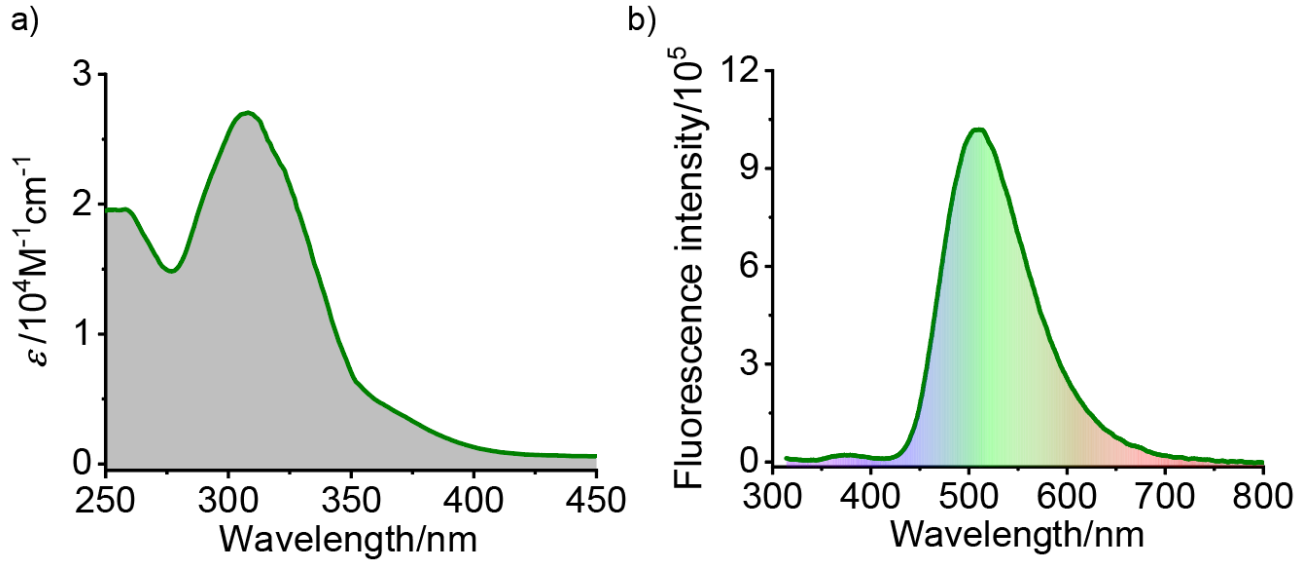

Figure S17. UV-vis absorption (a) and fluorescence spectra (b) of **2** in dichloromethane, c = $5x10^{-5}$ M. λ_{ex} = 309 nm.

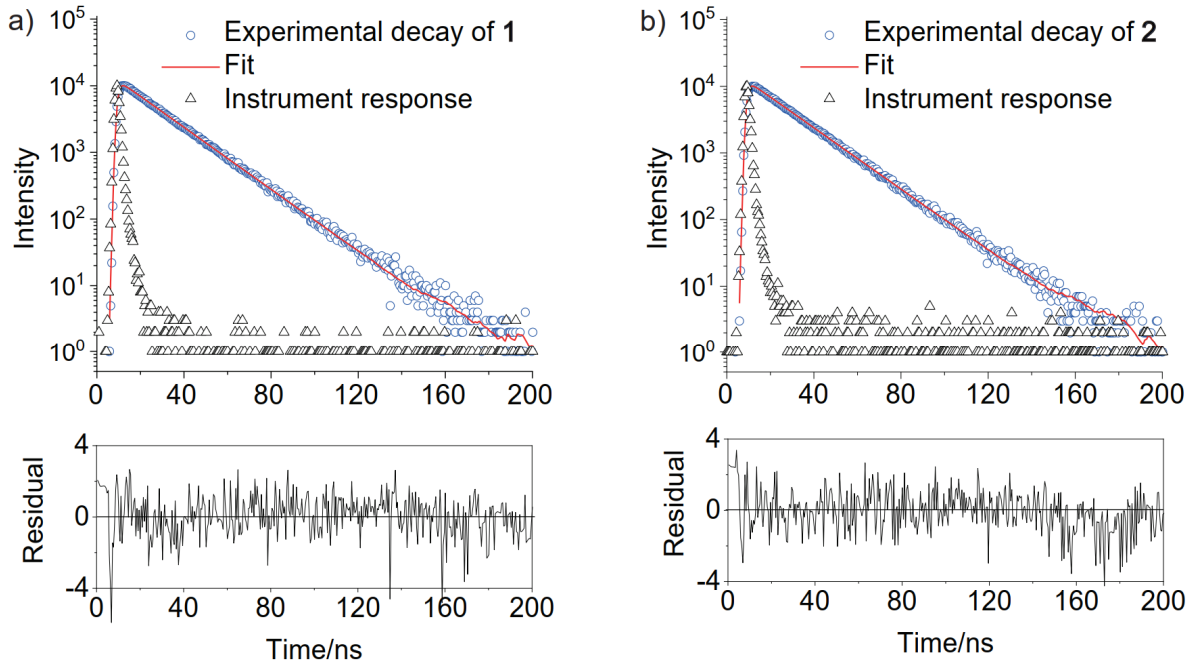

Figure S18. (a) Fluorescence decays of **1** in dichloromethane, Conc: $5x10^{-5}$ M, λ_{ex} = 294 nm, λ_{em} =508 nm. <τ> = 18.6 ns. (b) Fluorescence decays of **2** in dichloromethane, Conc: $5x10^{-5}$ M, λ_{ex} = 309 nm, λ_{em} =508 nm. <τ> = 18.8 ns.

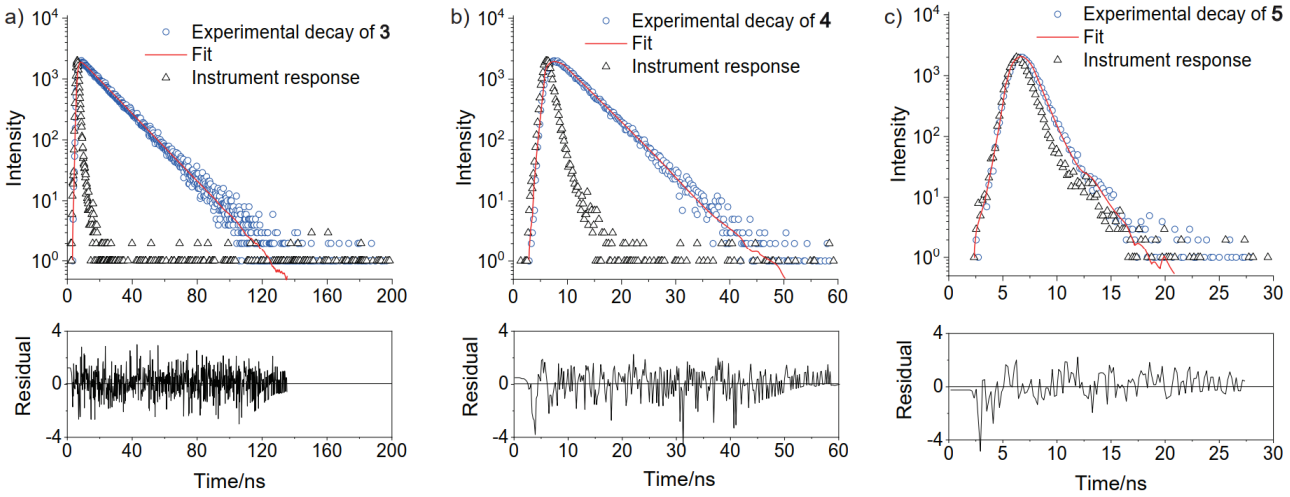

Figure S19. (a) Fluorescence decays of **3** in dichloromethane, Conc: $5x10^{-5}$ M, λ_{ex} = 350 nm, λ_{em} =508 nm. <τ> = 15.7 ns. (b) Fluorescence decays of **4** in dichloromethane, Conc: $5x10^{-5}$ M, λ_{ex} = 293 nm, λ_{em} =345 nm. <τ> = 4.8 ns. (c) Fluorescence decays of **5** in dichloromethane, Conc: $5x10^{-5}$ M, λ_{ex} = 307 nm, λ_{em} =370 nm. <τ> = 0.7 ns.

Table S2. UV-vis absorption and fluorescence emission spectroscopic data of donor-acceptors **1** and **2**, acceptor **3**, and donors **4** and **5**. Absorption and emission wavelength (λ_A and λ_F), extinction coefficient (ε), fluorescence lifetimes (τ) and quantum yields (Φ), Stokes shifts ($\Delta\lambda=\lambda_F - \lambda_A$).

Compounds	λ_A /nm	ε /$10^4 M^{-1}cm^{-1}$	λ_F /nm	<τ> /ns	Φ[a]	$\Delta\lambda$ /nm
1	294,340	2.40,0.96	508	18.6	0.63	214
2	311	2.73	508	18.8	0.26	197
3	350	0.53	508	15.7	0.50	158
4	293,340	2.10,0.47	346	4.8	0.29	53
5	307	2.30	371	0.7	0.03	64

[a] Relative fluorescence quantum yields were measured by using quinine sulfate in sulfuric acid aqueous solution (Φ=0.55) as reference.

Table S3. Fluorescence lifetimes of **1**-**5** in dichloromethane. [**1**] = [**2**] = [**3**] = [**4**] = [**5**] = 5×10^{-5}M. Fit: $A+B_1\exp(-t/\tau_1)+B_2\exp(-t/\tau_2)$.

Compounds	λ_{ex} /nm	λ_{em} /nm	τ_1/ns	Rel%	τ_2/ns	Rel%	χ^2
1	295	508	0.6	B_1=-0.172	17.2	B_2=0.108	1.04
	295	345	0.5	91.5	13.2	8.5	1.07
2	310	508	0.5	B_1=-0.174	17.0	B_2=0.114	1.09
	310	370	0.3	81.9	15.7	18.1	1.33
3	350	508	15.7	100			0.99
4	293	345	4.8	100			0.99
5	307	370	0.7	100			1.00

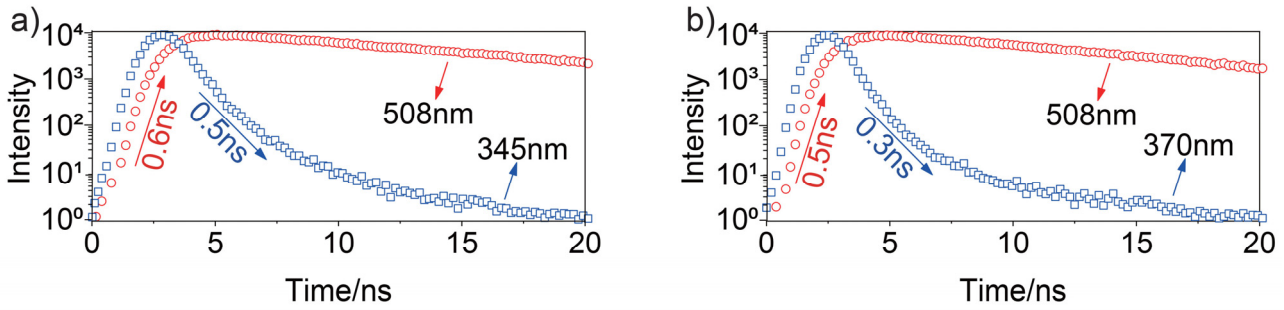

Figure S20. (a) Fluorescence decay curves of **1** at emission wavelengths of 345 nm (blue) and 508 nm (red), excitation wavelength = 295 nm. (b) Fluorescence decay curves of **2** at emission wavelengths of 370 nm (blue) and 508 nm (red), excitation wavelength = 310 nm.

5. Environmental-sensitive fluorescence probes

We investigated the environmental sensitivity of D-A **1** and **2** as novel fluorescence probes. The UV-vis absorption and emission spectra of **1** and **2** in various polarity solvents were measured (Figure S21 and Figure S22). With increasing solvent polarity, fluoresce emission of **1** or **2** shows gradual red shifts from 490nm to 530nm within visible light region (Figure S22a). Therefore, we can "see" the changes of their light-emitting colors from blue-green to yellow-green with increasing microenvironment polarity by naked eyes. In general, the emission wavelength of a chromophore is longer than its absorption wavelength, and the difference is called Stokes shift. Owing to intramolecular energy transfer, the Stokes shifts of **1** and **2** are very large (>180 nm, Table S4 and S5), which enable them become excellent candidate for fluorescence probes. The Stokes shifts of **1** and **2** increase with increasing solvent polarity (Δf). Stokes shift Δv ($\Delta v = v_A - v_F$) of **1** or **2** was plotted against polarity function Δf (Figure S22), which gives a steep slope, thus reveals a highly environment sensitivity of emission of **1** or **2**.

Table S4. Environment polarity sensitivity of D-A **1**. The stokes shifts (v_A-v_F or λ_F-λ_A) of **1** in various polar solvents. Absorption and emission wavelength (λ_A and λ_F). [**1**] = 5×10^{-5}M. Δf is a solvent parameter (orientation polarizability).

Solvents	Δf	λ_A /nm	λ_F /nm	v_A-v_F /cm^{-1}	λ_F-λ_A /nm
TL	0.0159	294	490	13605	196
Diox	0.0213	293	499	14090	206
$CHCl_3$	0.1445	294	504	14172	210
EtOAc	0.1998	292	504	14405	212
THF	0.2103	293	500	14130	207
CH_2Cl_2	0.2169	293	510	14522	217
n-BuOH	0.2642	293	522	14973	229
IPA	0.2770	292	524	15163	232
ACN	0.3066	292	525	15199	233
MeOH	0.3087	292	529	15343	237

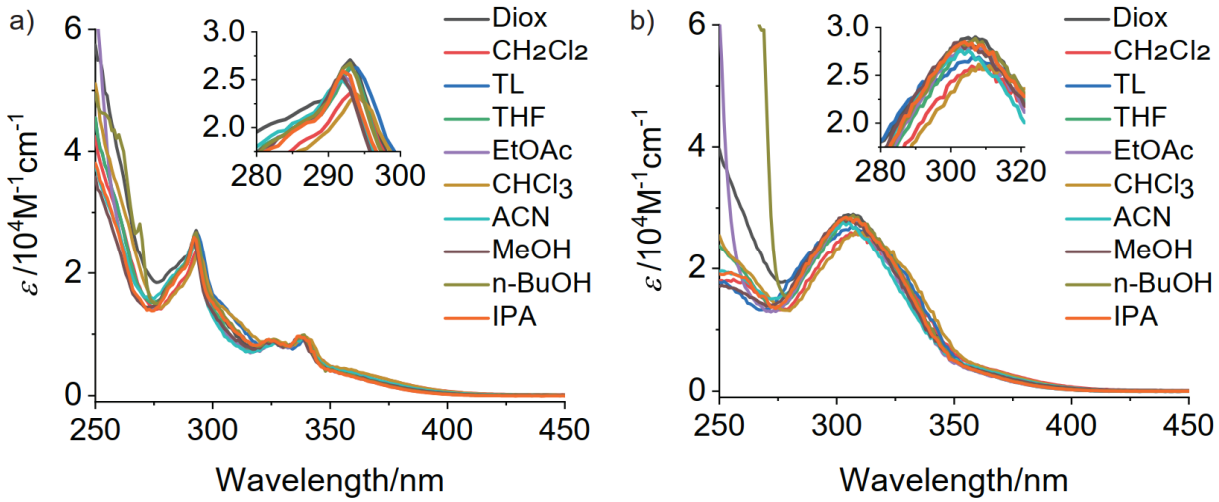

Figure S21. UV-vis absorption spectra of **1** (a) and **2** (b) in various polarity solvents: toluene (TL), 1,4-Dioxane (Diox), chloroform ($CHCl_3$), ethyl acetate (EtOAc), tetrahydrofuran (THF), dichloromethane (CH_2Cl_2), n-propanol (n-BuOH), iso-Propyl alcohol (IPA), acetonitrile (ACN), and methanol (MeOH). [**1**] = [**2**] = 5.0×10^{-5}M.

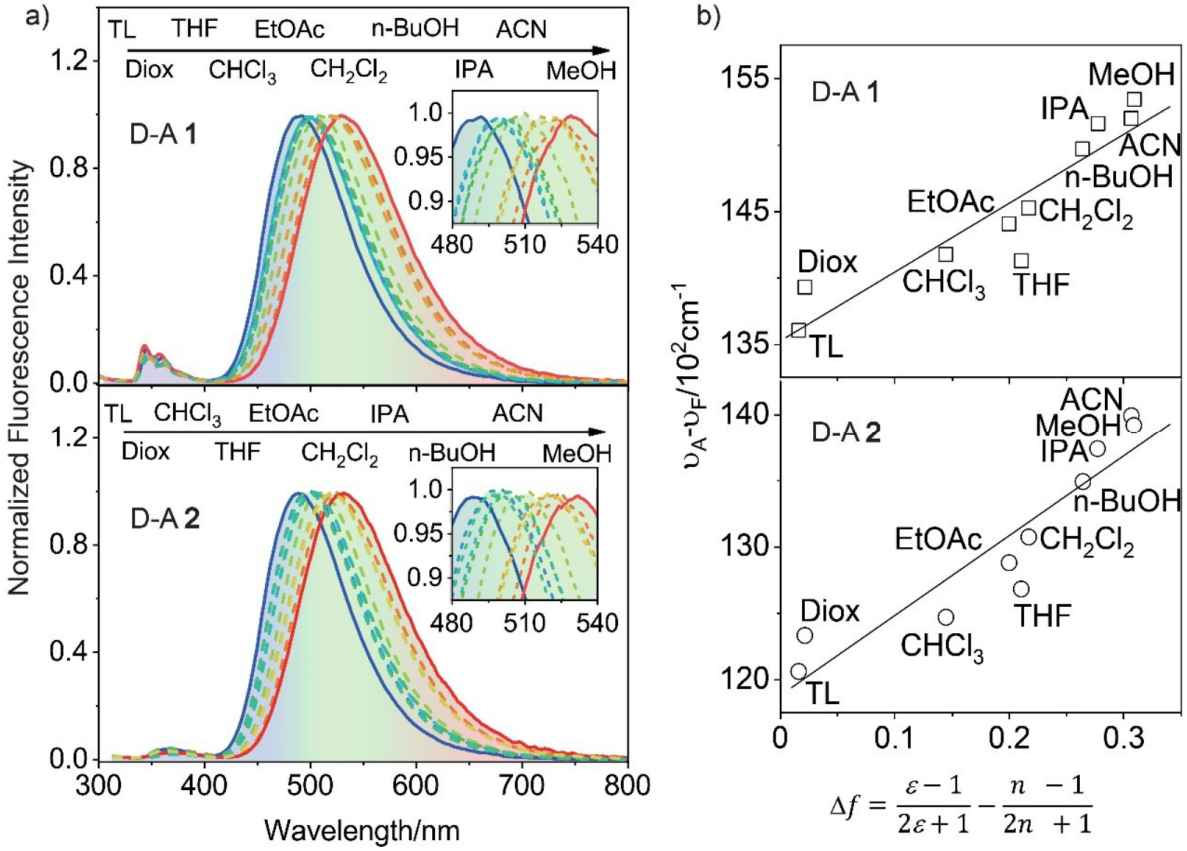

Figure S22. Environment-sensitive fluorescence probe properties. Fluorescence emission spectra of **1** and **2** in various polarity solvents: toluene (TL), 1,4-Dioxane (Diox), chloroform ($CHCl_3$), ethyl acetate (EtOAc), tetrahydrofuran (THF), dichloromethane (CH_2Cl_2), n-propanol (n-BuOH), iso-Propyl alcohol (IPA), acetonitrile (ACN), and methanol (MeOH). Excitation wavelengths are 294 nm and 309 nm for **1** and **2**, respectively, [**1**] = [**2**] = 5.0×10^{-5}M. (b) Changes in Stokes shifts ($\Delta\nu$) with increasing solvent polarity (Δf) for **1** and **2**.

Table S5. Environment polarity sensitivity of D-A **2**. The stokes shifts (ν_A-ν_F or λ_F-λ_A) of **2** in various polar solvents. Absorption and emission wavelength (λ_A and λ_F). [**2**] = 5×10^{-5}M. Δf is a solvent parameter (orientation polarizability).

Solvents	Δf	λ_A /nm	λ_F /nm	ν_A-ν_F /cm^{-1}	λ_F-λ_A /nm
TL	0.0159	308	490	12059	182
Diox	0.0213	307	494	12330	187
$CHCl_3$	0.1445	308	500	12468	192
EtOAc	0.1998	306	505	12878	199
THF	0.2103	306	500	12680	194
CH_2Cl_2	0.2169	306	510	13072	204
n-BuOH	0.2642	307	524	13489	217
IPA	0.2770	304	522	13738	218
ACN	0.3066	303	526	13992	223
MeOH	0.3087	305	530	13919	225

Environment-sensitive ability of **1** and **2** can be quantified by using the following equations:[3]

$$\Delta\nu = \nu_A - \nu_F = \frac{2}{hc}\Delta f \frac{(\mu_E-\mu_G)^2}{a^3} + \text{constant} \quad (1)$$

$$\Delta f = \frac{\varepsilon-1}{2\varepsilon+1} - \frac{n^2-1}{2n^2+1} \quad (2)$$

where h is the Planck's constant; c is the speed of light; ν_A and ν_F are the wavenumbers (cm^{-1}) of the absorption and emission, respectively; Δf is the orientation polarizability of solvent; μ_E and μ_G are the dipole moments of **1** and **2** in the excited and ground states, respectively; a is the molecular radius, which is calculated to be 13.0 and 13.6 Å for **1** and **2**, respectively.

According to the equations (1) and (2), we can calculate the change ($\Delta\mu$=μ_E-μ_G) in dipole moment between the excited and ground states of **1** or **2** from the slope of the fitting curve (Figure S22a). The values of $\Delta\mu$ are 35.6D and 40.7D for **1** and **2**, respectively. 35.6D and 40.7D are corresponding to the dipole moments that result from a unit charge separation of 7.42Å and 8.48Å, respectively. These results show that the excitation state dipole moments of **1** and **2** change significantly with the polarity of the solvent. We attributed it to high intramolecular energy transfer efficiency of **1** and **2**. These results reveals that **1** and **2** can be used as fluorescence probes with high microenvironment sensitivity properties.

6. Maleimide exchanges

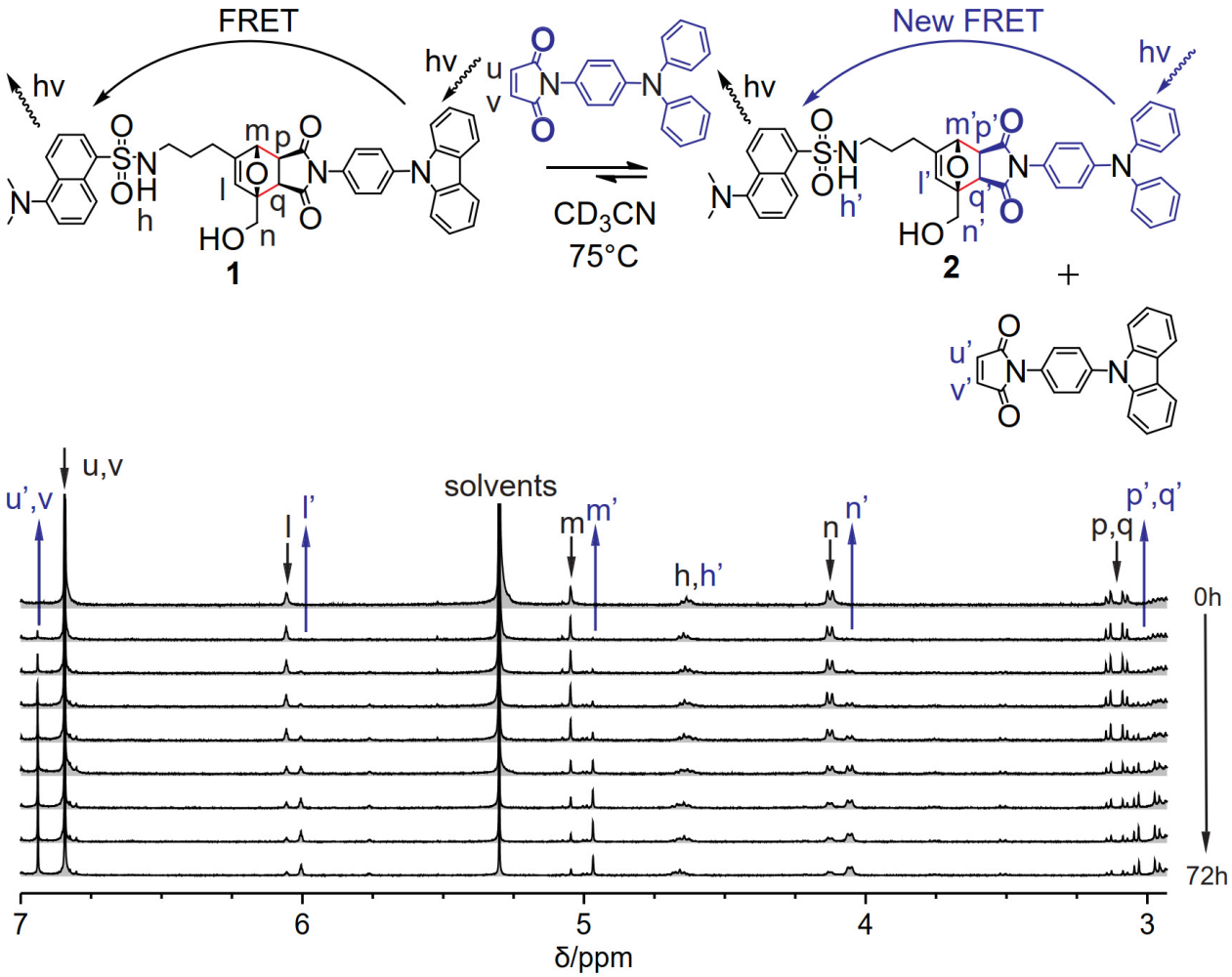

Figure S23. Exchange of maleimide groups in dynamic Diels–Alder covalent system in CD3CN at 75°C where **1** is converted into **2**. ^{1}H NMR spectral changes during the conversion of **1** into **2** in the dynamic Diels–Alder addition system. [**1**] = 0.025M, [Triphenylamine-based maleimide] = 0.075M. Reaction time = 0, 3, 6, 9, 12, 24, 36, 48, 72 h from top to bottom.

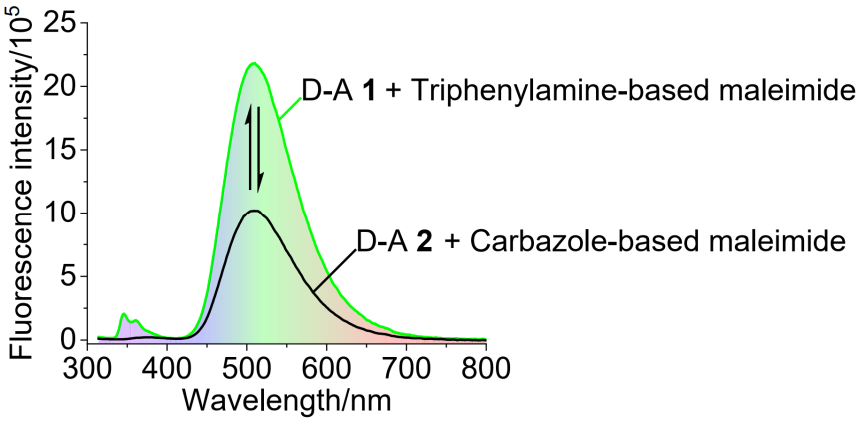

Figure S24. Reversible fluorescence changes during the maleimide exchanges for mutual conversion of **1** and **2**, Conc: $5x10^{-5}$ M, λ_{ex} = 307 nm.

7. References

[1] C. A. Parker and W. T. Rees, *Analyst*, 1960, **85**, 587-600.
[2] X. H. Li, Y. Wang, F. Li and X. Zhang, *Dyes Pigm.*, 2020, **182**, 108474.
[3] J. R. Lakowicz, *Principles of Fluorescence Spectroscopy*, Springer, New York, 2006, pp. 205-472.